Prod. Eng. Res. Devel. (2012) 6:11–18
DOI 10.1007/s11740-011-0355-5

PRODUCTION PROCESS

Effects on the deep drawing diagram in micro forming

F. Vollertsen

Received: 5 July 2011 / Accepted: 23 November 2011 / Published online: 2 December 2011

Abstract The limits of the processing window for deep drawing, collected in a deep drawing diagram, are affected by material behavior, process parameters and size effects. A size effect, more specific a density effect, explains the changes in forming behavior of foils with respect to the forming limit, denoted by the limiting drawing ratio. It is shown that it occurs in so called Tiffany structures. The changes in the tribology in deep drawing have an influence on the clamping limit of the processing window. The changes are induced by changes of the drawing speed. They can be explained by the lubricant pocket model only if one takes the temperature dependence of the viscosity of the lubricant into account.

Keywords Deep drawing · Process limits · Micro parts

List of symbols

μ	Coefficient of friction from Coulombs law
μ_{eff}	Effective coefficient of friction from numerical identification using the formula by Storoshew
$\mu_{ff}(p)$	Coefficient of friction as function of contact pressure, given by the so called friction function
μ_H	Coefficient of friction for hydrodynamic contact
μ_S	Coefficient of friction for solid contact
μ_T	Total coefficient of friction
A_0	Macroscopic contact cross section area (mm^2)
A_L	Liquid contact area (mm^2)
A_S	Solid contact area (also: real contact area) (mm^2)
d	Diameter (mm)
$d_{B,0}$	Initial blank diameter (mm)
d_p	Punch diameter (mm)
F	Force (N)
F_B	Blank holder force (N)
F_H	Normal force transferred by hydraulic medium (N)
F_N	(Total) normal force (N)
F_P	Punch force (N)
F_S	Normal force on solid contact (N)
l_p	Punch travel distance during forming process (mm)
p	(Contact) pressure (N/mm^2)
p_B	Blank holder pressure (N/mm^2)
$p_{B,0}$	Initial blank holder pressure (N/mm^2)
p_L	Lubricant pressure (N/mm^2)
p_S	Pressure of solid contact (N/mm^2)
r	Radius (mm)
r_D	Drawing radius (edge radius of drawing ring) (mm)
r_P	Punch radius (radius between bottom and mantle) (mm)
s_0	Sheet thickness (mm)
T	Temperature (K)
T_0	Temperature at viscosity η_0 (K)
v	Velocity (m/s)
v_P	Punch speed (m/s)
α	Viscosity temperature index
β	Drawing ratio (ratio of blank diameter to punch diameter)
β_{max}	Limiting drawing ratio
Δd_D	Drawing clearance (mm)
η	Viscosity (m^2/s)
η_0	Viscosity at temperature T_0 (m^2/s)
ρ	Density (g/cm^3)
φ_{max}	Maximum strain

F. Vollertsen (✉)
BIAS–Bremer Institut für angewandte Strahltechnik,
Klagenfurter Straße 2, 28359 Bremen, Germany
e-mail: vollertsen@bias.de

1 Introduction

A global aim of research is to understand the relations between properties and parameters and to present those to the user in industry in a convenient way. In sheet metal forming the deep drawing diagram is such a representation. While this is well known and understood in macro forming, there is a lack of information for the range of micro forming. According to [2] micro forming is used for those cases, where the size of the work piece is below 1 mm at least in 2 dimensions. The development of new products and the processes for its production is interfered by so called size effects, which make an adaption of the processes necessary. According to [31] size effects are defined as *deviations from intensive or proportional extrapolated extensive values of a process which occur, when scaling the geometrical dimensions*. The systematic approach of that paper was further developed in [32], which offers three main categories of size effects: The density, shape and structure effects, which are in turn divided into individual subgroups. This systematic, explained more in detail in [31] and applied to the area of micro forming in [34], can help to understand and to master these effects.

In sheet metal forming, the forming behavior is described using two characteristic diagrams, one is the forming limit diagram. It was introduced by Keeler and Backofen [17] and extended by Goodwin [4]. There is still research on it, e.g. on the determination of such diagrams [20]. Very early information about the influence of the sheet thickness on the forming limit diagram was given by Hasek and Lange [7], claiming that the forming limit is shifted to lower values, if the sheet thickness is decreased. However, this was shown for sheets of 1–2 mm made from steel. It was not clear whether this effect continues, if the sheet thickness is further reduced and if other materials like copper and aluminum are investigated. It will be shown in this paper that the decrease in formability with decreasing size in the micro range is a size effect out of the category of density effects.

The second process diagram is the deep drawing diagram. For the sake of clarity, the deep drawing diagram is shown schematically in Fig. 1, in order to define the characteristic lines named *wrinkling limit* (WL), *drawing limit* (DL), and *fracture limit* (FL). Very often, only one value, the *limiting drawing ratio* (LDR or β_{max}) is specified. This is the maximum value of the drawing ratio which can be achieved under the given conditions. It can occur that there is no drawing limit line and the LDR is defined by the intersection of the clamping limit and fracture limit.

In [30] it is shown that the LDR obtained from experiments with pure aluminum (Al 99.5) is reduced from 1.8 to 1.5 in lubricated deep drawing with punch diameter of 50

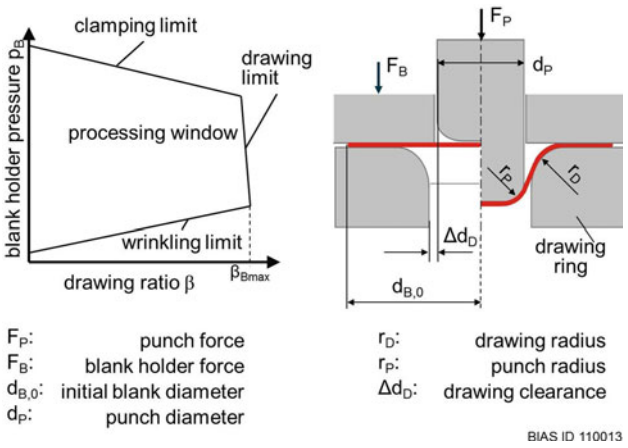

Fig. 1 Schematic deep drawing diagram

and 1 mm, respectively. The effects were explained by different size effects, where a localized flow phenomenon was suggested. By an investigation of the grain structure for Al- and Cu-foils of different thicknesses [12] it was shown that there is evidence for a strong local plastic deformation in thin foils, as only one grain covers the sheet thickness. This amplifies the localization of the flow behavior, as it is dominated by the orientation of the individual grain and not averaged by the influence of multiple grains like in polycrystals. Furthermore, it was shown in [12] that the LDR is reduced from 2.0 to 1.9 for copper, if the punch diameter is reduced from 5 to 1 mm. The discussion about the increase in scatter of the measured values, e.g. the punch force during deep drawing, was analysed by Justinger and Hirt [14]. The analysis showed that there is strong evidence for other sources of the scatter than the grain statistics at least for the punch force in deep drawing. This example shows the specific nature of the occurring size effects.

One essential key to size effects is the microstructure of the materials. As shown in [34], there are characteristic structures like polycrystals (e.g. there are many grains along the cross section of the material, yielding a material behavior like a continuum), oligocrytals (there are more than one grain along the cross section, but the number is too low to get a statistical averaging effect), and single crystals (no grain boundaries in the sample, the material behavior is strongly anisotropic). As there was no name for an essential structure of sheets, e.g. a structure having only one grain along the sheet thickness, but many grains along the in-plane-directions, the name ‘Tiffany structure’ was introduced [34], as that particular structure of glass handicrafts is very similar to that which was described for sheet metal. Tiffany structures show a strongly localized and uneven deformation behavior (see Fig. 2), what is due to

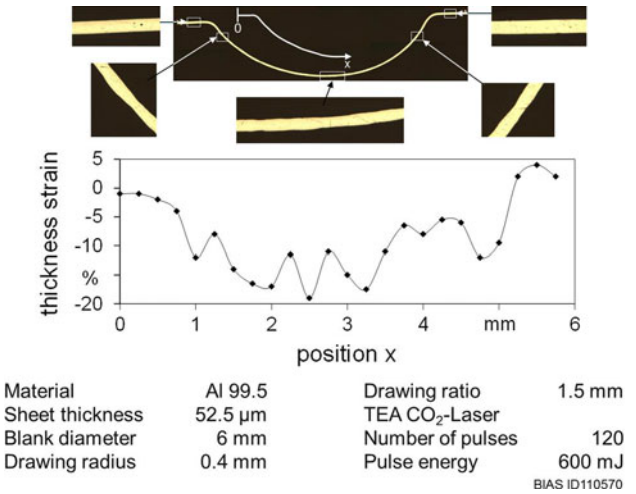

Fig. 2 Localized deformation in Tiffany structures [35]. In the case of a material behavior as a continuum, a continuous increase of the local strain towards the middle of the sample would be expected. Example is from deep drawing using laser induced shock waves

the dependence of the orientation of the particular grains concerning the loading direction; see e.g. [35].

2 Experimental

A direct driven high precision double acting press was used for the deep drawing at different speed. The design of the machine and details about the properties are explained in [25]. Further detailed information about the precision is given in [26].

All forming tools were made according to the rules of similarity (see e.g. [1]). The relative size of the main geometric parameters is given in Table 1. In order to address the actual size of the sample and experiment, the nomenclature 'sizeN' is used, where N is the sheet thickness or wire diameter in micrometer. For example, 'size20' addresses experiments using foils of 20 µm or wires with a diameter of 20 µm. According to Table 1 a punch diameter of 1 mm would apply for deep drawing in size20.

The sheet material was pure aluminum Al99.5 in the as delivered condition, the foil thickness was 20 and 100 µm. Deep drawing tools were made using tool steel 1.2379 (German standard), samples were lubricated with HBO (mineral oil) having a viscosity of 400 mm^2/s at 40°C.

Table 1 Dimensions of the deep drawing tools relative to the sheet thickness s_0 (20–100 µm) (see also Fig. 1)

Sheet thickness	Punch diameter d_P	Punch radius r_P	Drawing radius r_D	Drawing clearance Δd_D
s_0	50 s_0	5 s_0	6 s_0	1.4 s_0

The effective coefficient of friction μ_{eff} was determined by punch force measurements and the use of the formula for the maximum punch force from Storoshew (see [27] for the procedure, [29] for the formula). The friction function $\mu_{ff}(p)$, which accounts for the dependence of the coefficient of friction μ_{ff} on the contact pressure p, was determined according to [9].

3 Experimental results

The experimental results are already published elsewhere; see the citations at the figures; the most important experimental results are reprinted here for easier reading of the holistic discussion given here. Figure 3 shows the effective coefficient of friction, which is calculated from the maximum drawing force according to a calculation of the force from Storoshew. The method delivers an average value for the coefficient of friction and has the advantage that the effect of process variations (as punch speed variation) can be traced easily. The comparison of the two methods for the determination of the coefficient of friction (see e.g. [34]) showed that the intersection of the friction function μ_{ff} and the pressure-independent effective coefficient of friction μ_{eff} is essentially at the same contact pressure of 12 N/mm^2 for both sizes.

In Figs. 4 and 5 characteristic deep drawing diagrams for the size20 and size100 are given, demonstrating the changes with changes in size and drawing (punch) speed v_p. It is worth to note that there is an upward shift in the FL with increasing drawing speed, but no change to the DL for a constant size. The LDR β_{max} decreases with decreasing size.

4 Discussion

The number of grains per volume can be understood as a grain density, being the reason for categorizing the effect

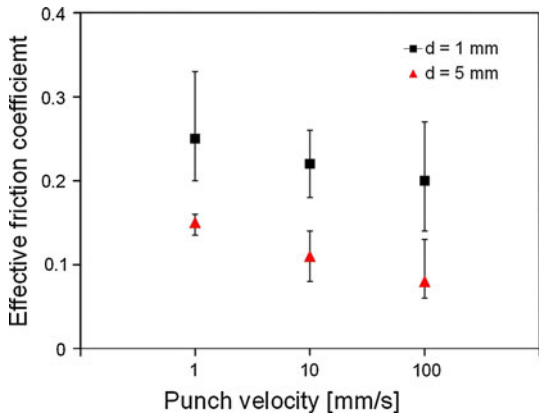

Fig. 3 Change of the effective coefficient of friction in deep drawing with different punch speeds [10]

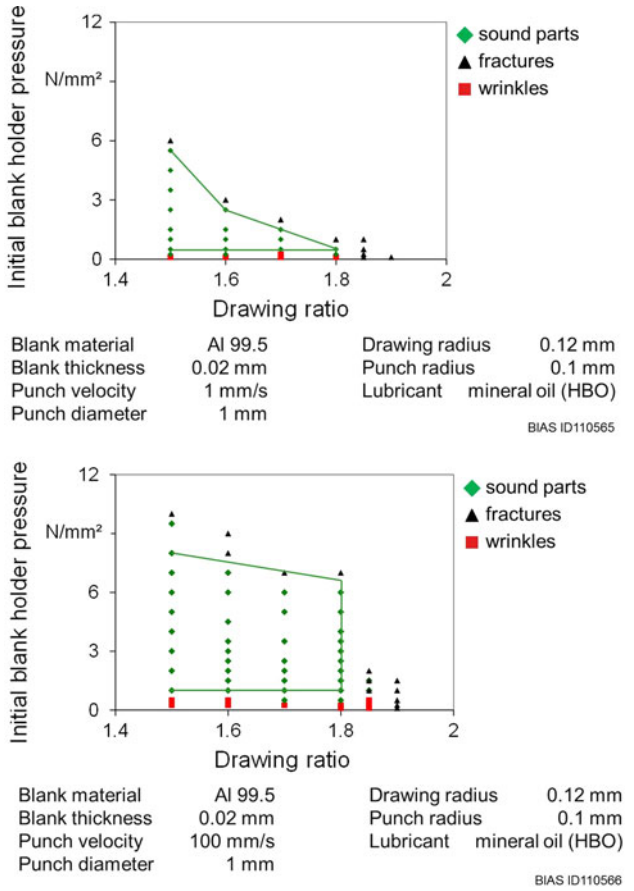

Fig. 4 Process window of deep drawing of size20 at different punch velocities [10]

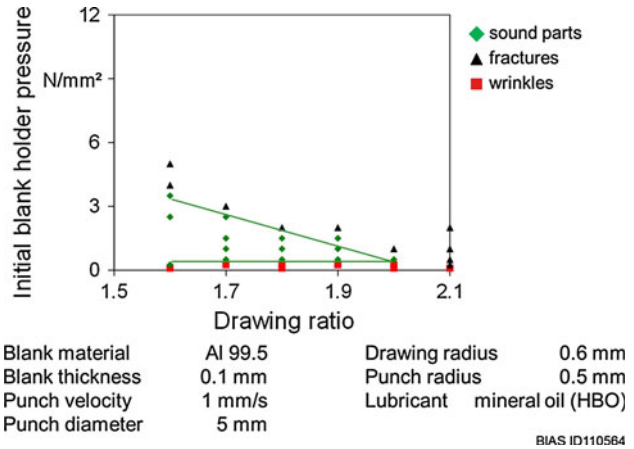

Fig. 5 Process window of deep drawing of size100 at low punch velocity [10]

of constant grain size (or in turn of constant grain density) into the category of density effects. Maintaining a constant grain size and reducing the dimension of the samples will lead to a change of the material structure from a polycrystalline to a Tiffany structure. Here it should be pointed out how the transition from polycrystalline to Tiffany structure changes the sheet forming behavior. In [13] the different strength behavior was discussed, but there are no data about the elongation to fracture. As shown in [10] the changes in the coefficient of friction due to changes in punch speed do not take influence on the drawing limit. In previous work it was assumed that local accommodation strains are responsible for the changes in the LDR [30] when changing the size. It appears to be correct that localized strain determines the LDR, but the reason for that has other roots. The basic reason is not a strain for accommodation to the local tool geometry, but the change in forming behavior due to the transition from polycrystalline to Tiffany structure. Such localization was observed in a bulge test for the deformation of 10 µm copper foil having a Tiffany structure, making further evaluation of the samples impossible [19]. It was shown in [33] using also a bulge test that the aluminum samples of size20 does not deform rotational symmetric as it is expected from FEM simulation with homogeneous microstructure. The uneven strain distribution is also maintained for different drawing speeds [11]. A metallographic analysis has shown that samples of size100 having a polycrystalline structure have a better forming behavior (according to the forming limit diagram) than samples of size20 having a Tiffany structure [12]. The Tiffany structure amplifies the localization of strain and an early failure (bottom fracture) occurs due to the excessive straining of single grains. Figure 6 shows schematically what happens: The critical part is the stretch drawn area at position A, which is located between the punch and the drawing ring at the beginning of the deep drawing process. According to the inferior deformation behavior of Tiffany structures, the forming limit line is shifted to lower strains with decreasing size. Due to that the forming limit in the stretch drawn area at position A is exhausted locally and bottom fracture set in earlier than expected from experience in the macro range. So the change in the LDR with size changes is a density size effect, which

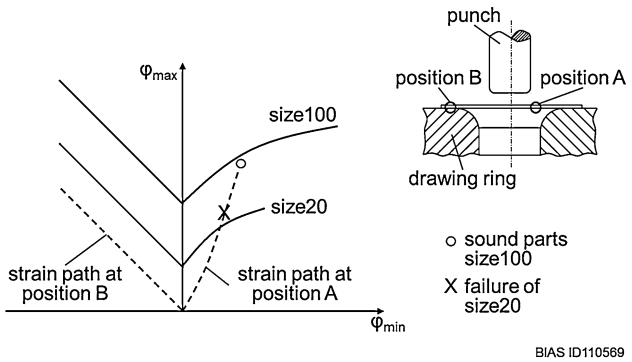

Fig. 6 Schematic limit drawing diagram with the size100 material showing continuum behavior and size20 showing Tiffany structure behavior

leads to a Tiffany structure and an accordingly material behavior.

While the density size effect based on Tiffany structures explains the influence on the LDR β_{Bmax} (see Fig. 1), the influence of the size of the work piece and the forming speed on the clamping limit cannot be attributed to that. Due to the fact that the drawing speed was increased, changes in material behavior like an increase of the flow stress or changes in the tribological behavior can be assumed.

First the assumption that there is a change in flow stress due to the high speed will be discussed which will show that those effects will not contribute to the observed changes. Despite the fact that 100 mm/s is a high punch speed, it can be easily calculated that the maximum deformation rate is less than 150 s^{-1}: The upper limit for the logarithmic strain φ_{max} occurring under the given conditions is taken from the change of the initial outer diameter $d_{B,0}$ (1.8 mm) to the punch diameter d_p (1 mm).

$$\varphi_{max} = \ln\left(\frac{d_p}{d_{B,0}}\right) \quad (1)$$

The lower limit for the processing time is taken from the minimum punch travel distance l_p, given by width of the initial flange:

$$l_p = (d_{B,0} - d_p)/2 \quad (2)$$

Division by the maximum punch speed (100 mm/s) yields the forming time (4 ms). Using the maximum deformation φ_{max} (from Eq. 1; i.e. 0.59) an upper limit of the deformation speed of 147 s^{-1} can be deduced. The real deformation rate will be even lower, as the punch travel distance for complete draw in will be larger than the initial flange width, but this is neglected as an upper limit consideration is intended. At a speed below 200 s^{-1} no change of the flow stress is expected. Therefore no effects from the material strength should occur. As changes in material behavior are excluded, the tribology appears to be the only feature to explain this shift, which enlarges the processing window. The changes in tribology have been already shown in [10], but the open question is the characteristic of its nature. Especially the changes in the coefficient of friction as shown in Fig. 3 must be explained. There are speed and size effects.

Figure 7 shows schematically the situation between tool (flat surface) and work piece (rough surface). The forming force is transferred by the individual contacts of the asperities with the contact area A_s for solid contacts. There is no reason why the tribology between such asperities, which is called *microtribology* throughout this paper, should change due to geometrical scaling of the sample, as the structure of the surface is considered to be constant. The reason must be looked up at the tribology of the whole contact area, comprising the microtribological contacts and the pockets in between them.

Very often a global statement is made that the lubricant pocket model (LPM) can explain the observed differences. This model, first qualitatively proposed by [21], is explained in detail in [28]. For the analysis made here, only the following should be pointed out, being a simplification of the further development of the LPM by Pfestorf [23]. This simplification is intentional to get an upper limit estimate for the effects. If lubricant is entrapped in the pockets between the asperity contacts, some fraction of the normal force F_N will be transferred also by the pressure in the liquid. This share is given by $p_L A_L$, where p_L is the pressure in the lubricant and A_L is the cross section covered by the (closed) lubricant pockets. An upper limit, neglecting open lubricant pockets, is given by

$$A_L = A_0 - A_S \quad (3)$$

where A_0 is the macroscopic cross section of the contact and A_S the sum of the solid contact areas, also known as real contact area.

As shown in Fig. 7 the liquid will escape from the lubricant pockets when reducing the overall size. This is so, because the distance to the border of the macroscopic contact area decreases, which in turn changes the nature of the lubricant pockets from closed to open ones. This is due to the fact that the structure of the surface is held constant during scaling. Therefore it is a structure effect, or more in detail a microgeometry effect (see e.g. [31] for definition)as the surface structure of the tool and the surface structure of the work piece are held constant, which results in a decrease of the number of closed lubricant pockets with decreasing size, see Fig. 7. As a consequence, the lubrication pockets are interconnected with the free boundary for the small sample, enabling the lubricant to escape quickly. It is also worth to note that the microtribology is assumed to stay unchanged.

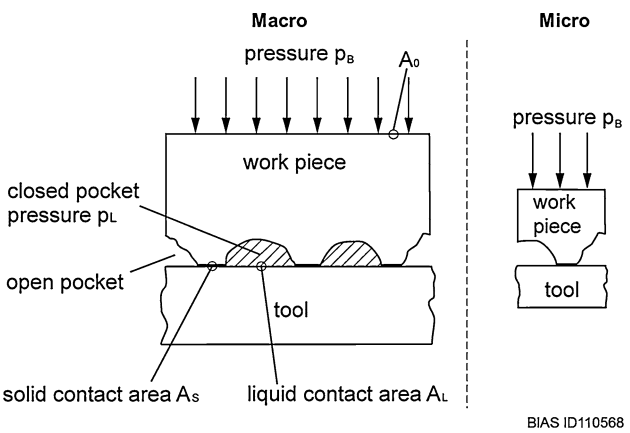

Fig. 7 Lubricant pocket theory for the coefficient of friction. The single solid contact spots are called 'microtribological contacts'

In order to get again an upper limit estimate for the difference between the size100 and size20 realization, the maximum difference between the contact pressures at the microtribological contacts should be pointed out. One should keep in mind that the macroscopic contact pressure is the same for both sizes.

The force transfer by the liquid, given by

$$F_H = p_L A_L \tag{4}$$

for the size100 will reduce to zero for the size20, as there are no closed lubricant pockets. As the normal force is composed from

$$F_N = F_H + F_S = p_L A_L + p_S A_S \tag{5}$$

the contact pressure at the microtribological contacts, e.g. the contact areas of the surface asperities, becomes:

$$p_S = (F_N - p_L A_L)/A_S \tag{6}$$

For the micro size, e.g. size20, the pressure p_L reduces to zero, so

$$p_S = F_N/A_S \tag{7}$$

This shows that the contact pressure p_s is bigger for the size20 than for size100, where Eq. 6 with $A_L p_L > 0$ gives the contact pressure.

If the LPM applies and no other effects are responsible for the size effect, the different coefficients of friction in macro and micro deep drawing should lie on a common Stribeck curve. From the conditions given in the experiments, the Stribeck number SN

$$SN = \frac{\eta v}{p_S} \tag{8}$$

is in the range of 1.9 mm^5/Ns^2 to 3,300 mm^5/Ns^2. According to [5], who made experiments using motor oil at comparable conditions, this is in the range of mixed lubrication below the transition to hydrodynamic lubrication. This can explain the decrease of the coefficient of friction with increasing sliding speed.

It is postulated that the Stribeck curve applies to the microtribological contacts. In that case it is obvious that the difference between the two sample dimensions (1 mm and 5 mm punch diameter) is given from the LPM as a difference of the pressure p_S. The upper limit for the pressure of the entrapped lubricant p_L is given by the contact pressure p_S to ensure sealing of the pockets. In order to calculate the upper limit of the load transferrable by the lubricant, a pressure

$$p_L = p_S \tag{9}$$

is taken. The second parameter is the fraction of the lubricant pocket area, given by Eq. 3. The real contact area can be determined experimentally, see e.g. [3]. An application of that method showed the strong influence of the contact load, sliding distance, and other parameters, but a minimum of 0.05–0.1 A_0 seemed reasonable [24].Other work showed a real contact area of some 0.5 for low loads [23], which is consistent with the simulation of the contact area by Hol et al. [8]. In order to get an estimate for the lower limit of the Stribeck number, a value of 0.05 A_0 is taken for A_S. As the lubricant in experiments with size100 is assumed to transfer the same pressure as the solid contact, the microtribological contact pressure p_S is equal to the nominal pressure. From [34] a nominal pressure of 12 N/mm^2 seems to be the average at the moment of the determination of the coefficients of friction by the method using the Storoshew equation. From those values the Stribeck number for size100 ranges from 33 mm^5/Ns^2 to 3,300 mm^5/Ns^2 for the lowest and highest drawing speed, respectively.

For size20, the lubricant pressure in the lubrication pockets is assumed to be zero to get the lower limits of the Stribeck number. As the real contact area has to transfer the whole load, the effective pressure $p_{S,size20}$ is increased to 240 N/mm^2. Despite the fact that this value is far above the flow stress of the sample material it is taken to calculate the lower limit of the Stribeck number. This results in Stribeck numbers of 1.9 mm^5/Ns^2 to 165 mm^5/Ns^2. When redrawing the results from Fig. 3 in Fig. 8 as a Stribeck curve, there is a clear overlap of the two curves for size20 and size100 with different coefficients of friction. It can be concluded that the LPM cannot explain the whole size effect as measured. An additional factor of at least 10 has to be explained by a further effect.

So far, the same viscosity was taken for all calculations, but it is well known that there is a very strong influence of the temperature T on the viscosity η of lubricants, which can be described by an exponential law (see e.g. [6]):

$$\eta = \eta_0 e^{-\alpha(T-T_0)} \tag{10}$$

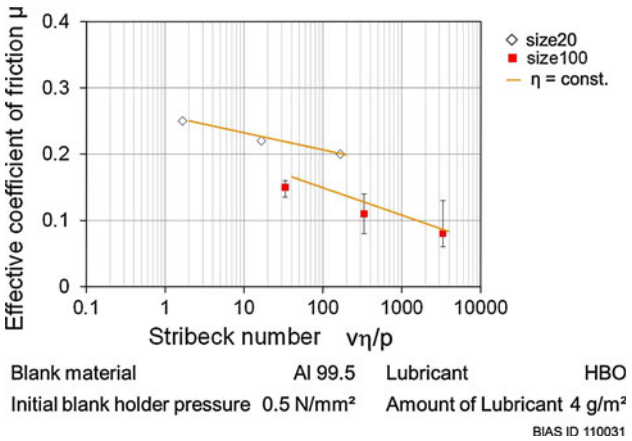

Fig. 8 Stribeck curve for different sizes

where η_0 is the viscosity at temperature T_0 and α as the viscosity-temperature-index. Typically, a temperature increase of 80 K decreases the viscosity of lubricants by a factor of 100. So even a smaller heating of the lubricant could explain the missing factor of 10.

There are three effects which take influence on the temperature difference of the lubricant for size20 and size100:

1. For size100 there is more lubricant kept in and around the microtribological contact zone, as the lubricant cannot escape from the closed lubricant pockets. If the same amount of heat per contact area is generated, the temperature increase will be less for size100 than for size20.
2. The frictional heat is generated as heat per area. As the thickness of size100 samples is larger, these samples might act more effectively as heat sinks. Due to that, heating of the lubricant should be less for size100 than for size20.
3. As explained above, the local contact pressure is larger for size20 than for size100. This will lead to a more pronounced heat generation for size20 than for size100.

All of the listed effects will lead to a stronger heating of the lubricant for size20 compared to size100, while the third effect is probably the strongest one. A quantitative estimate of the temperature increase will be very difficult to make, so only qualitative estimates are given.

Heating effects in sheet metal forming are investigated rarely. From simulation and experiments a maximum heating of only less more than 5 K were detected in an Erichsen test of a steel sheet having a thickness of 0.8 mm [22]. For a stamping process with larger sliding distances than in an Erichsen test a local temperature increase of more than 60 K was identified by simulation [18]. According to [15] the temperature rise during deep drawing of cups from brass with a diameter of 1–8 mm at a punch speed of 100 mm/s was calculated to be 70–190 K. A detailed description of the calculation and the simplifications made are described in [16]. From industrial experience it is also known that the temperature of the tools can rise by some 100 K during deep drawing. As the transition temperature during deep drawing might be even higher it seems feasible that there is a difference in the temperature of the lubricant of 30 K between size20 and size100 which would result in a difference of the viscosity by a factor of 10 explaining the necessary order of magnitude for the Stribeck number. Therefore a structure size effect, described by the LPM augmented by a consideration of the temperature dependent viscosity and different heating at different dimensions could explain the observed effects. As a result, Fig. 9 shows the Stribeck curve when using temperature-corrected values of the Stribeck number.

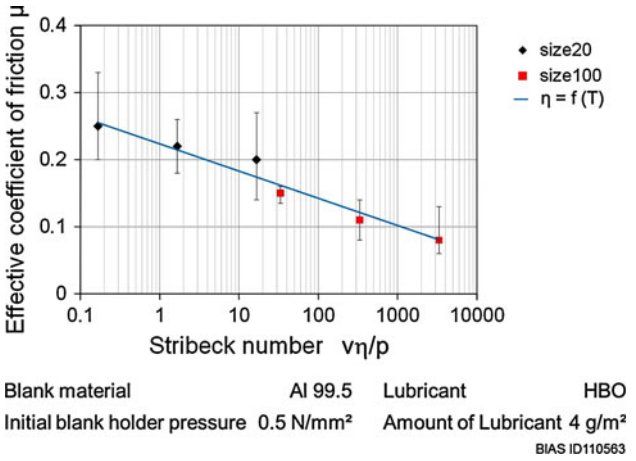

Fig. 9 Stribeck curve for different sizes and speeds when considering a temperature effect on the viscosity

5 Conclusions

- The size dependent influence of the speed on the clamping limit of the deep drawing diagram can be explained by the change of the tribological behavior. The microtribology which takes place at the contact of individual asperities can be considered as constant for the different conditions. The effect can be explained using the model of open and closed lubrication pockets, but is consistent only if one takes the temperature dependent viscosity of the lubricant and different heating during the processes into account.
- The size effect on the LDR is probably a result of the changes in flow behavior, which results from the transition of a true polycrystalline material to a Tiffany structure (having essentially only one grain in thickness direction). According to that explanation there should be no influence of the forming speed on the LDR, as it was observed.

6 Outlook

Further work has to be done, if the heating of the lubricant should be taken into account for the friction behavior during (micro) deep drawing. This would be a very large challenge for a multi scale simulation, as the thermal conductivity, the fluid dynamics of the lubricant and the heat flow in the tool and workpiece has to be described in addition to the (macroscopic) plastic flow of the material. Otherwise, size,

velocity and pressure dependent coefficient of friction have to be measured and implemented in simulation.

Acknowledgments The author is grateful for the financial support of the Deutsche Forschungsgemeinschaft (DFG) of the projects B1 and B3 of the Collaborative Research Center SFB 747, where the results were obtained. The author also thanks for support by Dipl.-Ing. S. Grünenwaldand Dr.-Ing. Z. Hu whilepreparingthismanuscript.

References

1. Dahl W, Knopp R, Pawelski O (1993) Umformtechnik Plastomechanik und Werkstoffkunde (in German). Springer, Berlin, pp 158–173
2. Geiger M, Kleiner M, Eckstein R, Tieseler N, Engel U (2001) Microforming. CIRP Annal Manufact Technol 50(2):445–462
3. Geiger M, Engel U, Vollertsen F (1992) In situ ultrasonic measurement of the real contact area in bulk metal forming processes. CIRP Annal Manufact Technol 41(1):255–258
4. Goodwin GM (1968) Application of strain analysis to sheet metal forming problems in the press shop. SAE paper 680093
5. Grebe M, Feinle P (2004) Reibwertuntersuchungen an Motorölen im Mikrotribometer (in German) Tribologie-Fachtagung, Reibung, Schmierung und Verschleiß Göttingen
6. Grote K-H, Feldhusen J (2001) Dubbel Taschenbuch für den Maschinenbau (in German). Springer, Berlin, p E84
7. Hasek V, Lange K (1980) Forming-limit diagram and its applications in deep-drawing and stretch-forming processes (in German). Wirtsch Z Ind Fertig 70:577–580
8. Hol J, Cid Alfaro MV, de Rooij MB, Meinders T (2010) Multiscale fritction modeling for sheet metal forming. In: Felder E, Montmitonnet P (eds) 4th International conference on tribology in manufacturing process (ICTMP 2010). Transvalor Paris, pp 573–582
9. Hu Z, Vollertsen F (2004) A new friction test method. J Technol Plasticity 29(1–2):1–9
10. Hu Z, Vollertsen F (2010) Effect of size and velocity dependent friction in deep drawing on the process window. In: Felder E, Montmitonnet P (eds) Proceedings of the 4th International conference on tribology in manufacturing processes (ICTMP (2010)). Transvalor Paris, pp 583–592
11. Hu Z, Wielage H, Vollertsen F (2010) Effect of strain rate on the forming limit diagram of thin aluminum foil. In: Dohda K (ed) Proceedings of the International forum on micro manufacturing (IFMM'10). Nagoya Institute of Technology Nagoya (2010), pp 181–186
12. Hu Z, Wielage H, Vollertsen F (2011) Forming behavior of thin foils. In: Duflou JR, Clarke R, Merklein M, Micari F, Shirvani B, Kellens K (eds) 14th International conference on sheet metal (SheMet11). TransTech Publication, Zurich-Durnten (2011), pp 1008–1015
13. Janssen PJM, de Keijser ThH, Geers MGD (2006) An experimental assessment of grain size effects in the uniaxial straining of thin Al sheet with a few grains across the thickness. Mater Sci Eng A419:238–248
14. Justinger H, Hirt G (2007) Scaling effects in the miniaturisation of the deep drawing process. In: Vollertsen F, Yuan S (eds) International conference on new forming technologies (2nd ICNFT'07). BIAS-Verlag Bremen, pp 167–176
15. Justinger H, Hirt G (2007) Analysis of size effects in the miniturized deep drawing process. Key Eng Mater 344:791–798
16. Justinger H (2009) Experimentelle und numerische Untersuchung von Miniaturisierungs-einflüssen bei Umformprozessen am Beispiel Tiefziehen (in German). Shaker Verlag
17. Keeler SR, Backofen WA (1963) Plastic instability and fracture in sheets stretched over rigid punches. Trans ASM 56:25
18. Kim H, Han S, Yan Q, Altan T (2008) Evaluation of tool materials, coatings and lubricants in forming galvanized advanced high strength steels (AHSS). CIRP Annal Manufact Technol 57:299–304
19. Kim J, Hoffmann H, Golle M, Golle R (2009) Untersuchungen zum Werkstoffverhalten von sehr dünnen Kupferblechen (in German). In: Vollertsen F (ed) Größeneinflüsse bei Fertigungsprozessen. BIAS Bremen, pp 57–78
20. Merklein M, Kuppert A, Geiger M (2010) Time dependent determination of forming limit diagrams. CIRP Annal Macufact Technol 59(1):295–298
21. Pawelski O, Lueg W (1961) Versuche und Berechnungen über das Ziehen und Einstoßen von Rundstäben (in German). Stahl u. Eisen 81(25):1729–1739
22. Penazzi L, Yang G, Levaillant C, Le Floch A (1996) Assessment of thermal effect in the sheet metal forming process. 19th IDDRG Biennial Congress, pp 287–293
23. Pfestdorf M (1997) Funktionale 3D-Oberflächenkenngrößen in der Umformtechnik (in German). Meisenbach Verlag, Bamberg
24. Putz A (2006) Grundlegende Untersuchungen zur Erfassung der realen Vorspannung von armierten Kaltfließpresswerkzeugen mittels Ultraschall (in German). Meisenbach Verlag, Bamberg, p 85
25. Schulze Niehoff H, Vollertsen F (2007) Versatile microforming press. In: Vollertsen F, Yuan S (eds) International conference on new forming technologies (2nd ICNFT'07). BIAS-Verlag, Bremen, pp 167–176
26. Schulze Niehoff H (2008) Entwicklung einer hochdynamischen, zweifachwirkenden Mikroumformpresse (in German). BIAS-Verlag, Bremen
27. Schulze Niehoff H, Hu Z, Vollertsen F (2008) Einflüsse von Größeneffekten auf das Grenzziehverhältnis In: Steinhoff K, Kopp R (eds) Der Pawelski—Umformtechnik im Spannungsfeld zwischen Plastomechanik und Werkstofftechnik. Hrsg. GRIPS media GmbH Bad Harzburg, pp 207–215
28. Sobis T, Engel U, Geiger M (1992) A theoretical study of wear simulation in metal forming processes. J Mater Process Technol 34:233–240
29. Storoschew MW, Popow EA (1968) Grundlagen der Umformtechnik. VEB Verlag Technik, Berlin
30. Vollertsen F, Hu Z (2007) On the drawing limit in micro deep drawing. J Technol Plasticity 32(1/2):1–11
31. Vollertsen F (2008) Categories of size effects. Product Eng 2(4):377–383
32. Vollertsen F, Biermann D, Hansen HN, Jawahir IS, Kuzman K (2009) Size effects in manufacturing of metallic components. CIRP Annal Manufact Technol 58(2):566–587
33. Vollertsen F, Hu Z, Wielage H, Blaurock L (2010) Fracture limits of metal foils in micro forming. In: Hinduja S, Li L (eds) 36th International MATADOR conference. Springer, London, pp 49–52
34. Vollertsen F (2011) Size effects in micro forming. In: Duflou JR, Clarke R, Merklein M, Micari F, Shirvani B, Kellens K (eds) 14th International conference on sheet metal (SheMet11). TransTechPublication, Zurich-Durnten, pp 3–12
35. Wielage H (in print) Hochgeschwindigkeitsumformen durch laserinduzierte Schockwellen. Series Strahltechnik, BIAS, Bremen